Proceedings of the
44th IEEE Conference on Decision and Control, and
the European Control Conference 2005
Seville, Spain, December 12-15, 2005

Lateral control of autonomous electric cars for relocation of public urban mobility fleet

Stefano Malan, Mario Milanese
Dipartimento di Automatica e Informatica
Politecnico di Torino, Torino, Italy
Email: stefano.malan@polito.it, mario.milanese@polito.it

Pandeli Borodani, Alessandro Gallione
Vehicles Department, Vehicle Control Systems
Centro Ricerche FIAT, Orbassano (TO), Italy
Email: pandeli.borodani@crf.it, alessandro.gallione@crf.it

Abstract— **This paper deals with lateral dynamic control of electric vehicles in a urban environment, motivated by individual public transportation issues, aimed to reduce metropolitan areas pollution. The framework in which the control strategy is developed is the so-called "Look-Down Reference", where the lateral displacement is obtained from a on board sensor, interacting with a road infrastructure. In this framework, the designed control algorithm is made up of three nested closed loops with cascade compensators, where the outer one is nonlinear. Results from experimental tests performed on an actual circuit show the effectiveness of the considered control strategy.**

I. INTRODUCTION

In the last decades, one of the most important studied problems, in metropolitan areas, is the limitation and prevention of pollution caused by the increasing private traffic. Many cooperative actions have to be taken to afford and solve this problem. One of them is to implement electric car fleet, to be rented for individual public transportation. For this solution, several parking areas have to be distributed around the metropolitan area, in correspondence to other transportation system terminals, such as railway stations or bus terminals, to public buildings, to firm offices, etc., to locate the electric cars, used to move in the same area. One of the problems that arises in managing this car fleet is the automatic redistribution of cars among the different parking areas. This task could be accomplished in a manual way by single workers, but, in this case, there will be no economic convenience. Consequently, an automatic redistribution has to be considered and an automatic driving problem arises.

In the above described context, small platoons ($1 \div 5$ units) of cars have to move autonomously along a pre-defined path, for example a dedicated lane, from a crammed parking area to an empty (or almost empty) one. This way, longitudinal and lateral vehicle dynamic control problems have to be considered and solved, to allow the automatic transfer of cars, as well as multiple stop & go problem, interaction with road infrastructure such as traffic lights and signals, etc.

In the last few year, many paper dealt with the lateral control problem in different contexts (urban or highway), considering different sensors/infrastructure conditions (road markers or GPS positioning signal) and many different control strategies.

An overview of different control strategies both in longitudinal and lateral control can be found, for example, in [1] and following the references therein. In particular, considering lateral control, the "Look-Down Reference" case is the one considered in our paper.

Also in the California Program on Advanced Technology for the Highway (PATH) both longitudinal and lateral control are considered; see, for example, [2], where vehicle dynamic models, interaction with sensors system and control issue are discussed in details.

On the contrary, the urban environment is taken into account in [3], facing with both longitudinal and lateral control problems.

The particular problem of lateral control with respect to a marked lane is considered in [4] and in [5]. Moreover, in [5] a comparison between automatic and human driving is presented.

Both GPS and road markers, together with nonlinear vehicle models are considered in [6] for measuring vehicle position in emergency situations.

At last, a comparison between four different control strategies can be found in [7] for the lateral control problem.

In this paper we consider the totally autonomous lateral control problem, in a urban environment, with lateral displacement information obtained from a road infrastructure. This problem was afforded in [8], where a difficult due to physical constraints not allowing a perfect road markers placement was pointed out. Here we present a possible algorithmic solution, not requiring real-time computation, to overcome this problem without changing the road infrastructure.

II. PROBLEM FORMULATION

The plant to be controlled is a FIAT 600 "Elettra", equipped with an electric engine and suitable actuator and sensors; a road infrastructure, used to determine the lateral position of the vehicle, can be also considered as a part of the plant.

The overall system layout is resumed in Fig. 1, where the plant block includes actuator and sensors. The actuator is an electrical steering servo system, which input is the requested torque T_v. Three sensors are available to measure the steering wheel angle δ_v, the vehicle yaw rate $\dot{\Psi}$ and the vehicle lateral displacement Y_s with respect to the vehicle desired path. This last measure is obtained through an antenna, mounted on the vehicle, able to interact with transponders "drowned" into

0-7803-9568-9/05/$20.00 ©2005 IEEE

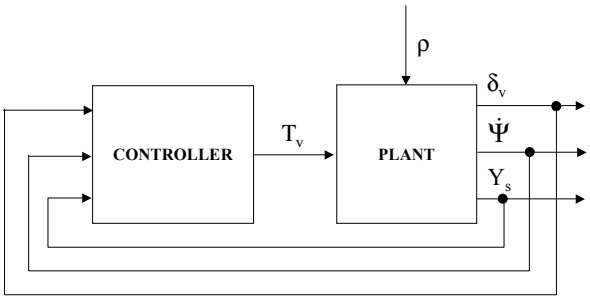

Fig. 1. System layout.

the road. The vehicle actuator and sensors here considered are the ones used for the lateral control task. Of course other devices used in the longitudinal control task are present, such as braking and accelerating actuators and distance sensor (radar).

Note that, while δ_v and $\dot{\Psi}$ signals are measured at a chosen sampling rate of 10 ms, the displacement Y_s can be measured only when the vehicle pass over a transponder. The transponders are placed at a distance of one (on a bend) or two (on a straight) meters, so this last measure is intrinsically discrete, with a sampling time of about 0.5÷1 s, varying with vehicle speed.

Moreover, the lateral displacement Y_s is given by the vehicle dynamic and by the track that the vehicle has to follow, which can be conveniently described through its curvature ρ. As indicated in Fig. 1, the curvature signal acts as a disturbance in the control structure.

The plant can be decomposed in three parts: the actuator, the vehicle dynamic and the sensor, as depicted in Fig. 2. These three parts are modelled as follows.

The actuator is described by a second order transfer function:

$$G_a(s) = \frac{K_a}{1 + \frac{2\zeta_a s}{\omega_a} + \frac{s^2}{\omega_a^2}} \tag{1}$$

which static gain K_a ranges between 0.15 and 2.5, and which poles are complex with natural frequency ω_a between 2 and 5 and damping ζ_a between 0.45 and 1. This parameters variation depends nonlinearly on the vehicle velocity V_s and on the input torque T_v values.

To describe the vehicle dynamic the well known single track model (see, for example, [9]) can be conveniently used. Moreover, knowing that the vehicle speed here considered ranges between 0 and 20 km/h, and using experimental data, it can be seen that a static model, obtained from stationary conditions applied to the single track model, is able to describe very well the vehicle behavior.

This way, a linear static model, which gain depends nonlinearly from the vehicle speed V_s, was used:

$$\dot{\Psi} = K\left(V_s\right) \cdot \delta_v \tag{2}$$

where the gain $K\left(V_s\right)$ is given by:

$$K\left(V_s\right) = \frac{V_s}{p_1 + p_2 \cdot V_s^2} \tag{3}$$

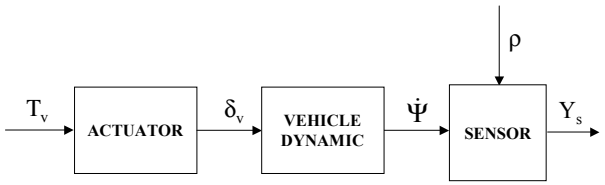

Fig. 2. Plant description.

with $p_1 = 38$ m and $p_2 = 0.7$ s^2/m, obtained from experimental data.

In Fig. 3, the time behavior of the acquired yaw rate (solid line) and simulated, using model (2), yaw rate (dash-dotted line) are compared. It can be seen that the static model given by (2) and (3) is quite accurate.

At last, the sensor description can be obtained by simple geometric considerations, as described, for example, in [10]:

$$Y_s = G_{1s}(s, V_s)\dot{\Psi} - G_{2s}(s, V_s)\rho \tag{4}$$

where

$$G_{1s}(s, V_s) = \frac{(1.7 - 0.007V_s^2)s + V_s}{s^2} \tag{5}$$

$$G_{2s}(s, V_s) = \frac{V_s(0.4s + V_s)}{s^2} \tag{6}$$

The numeric values in (5) are obtained using the same procedure above described for the vehicle dynamic model given by (2) and (3), while the numeric value 0.4 in (6) is the distance between the antenna and the front axle.

According to the presented plant description and desired behavior, the main control specification is formulated in these terms: the vehicle has to follow the desired path, a priori known, given by road markers (the transponders), with an error (the lateral displacement Y_s) not greater than the car mounted antenna measure range (± 0.25 m), and, possibly, for robustness reasons, not greater than about half of the

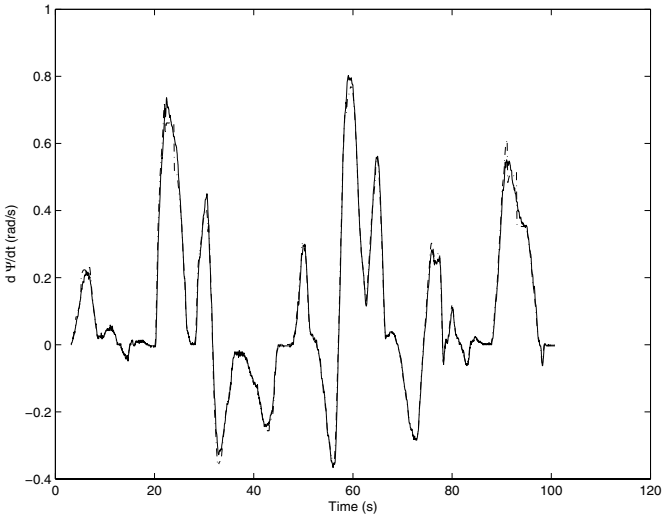

Fig. 3. Acquired (—) and simulated (---) yaw rate.

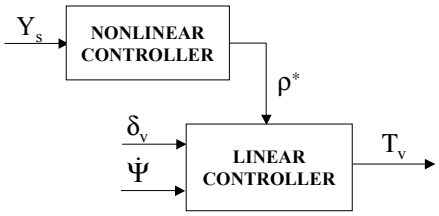

Fig. 4. Controller layout.

antenna measure range (say $\pm$ 0.1 m), with a limited control effort of 7 Nm maximum, that takes into account an actual saturation on signal T_v.

III. CONTROL ALGORITHM

The overall control algorithm (controller block of Fig. 1) can be decomposed in two main parts: a linear and a nonlinear controller, as described in Fig. 4. Moreover, in the same figure, it is evidenced that the variables δ_v and $\dot{\Psi}$ are the feedback signals for the linear controller, while the lateral displacement Y_s is the feedback signal for the nonlinear one.

The nonlinear controller $\rho^* = C_{nl}(Y_s)$ works as a combined feedforward/feedback control structure. In facts, see Fig. 5, it computes the corrected curvature ρ^* as the inverse of the radius of a circle that pass through the absolute positions, that are known, of the next two path markers T_1 and T_2 and from the present absolute position of the vehicle V_p. The vehicle position can be simply computed on the base of the measured lateral displacement Y_s, the a priori known transponders T_0 and T_1 positions and distance d_{01} between present and next transponder, and with the simplifying hypothesis that the angle α measures 90 degrees. The a priori known absolute positions of the path markers give the *feedforward* information, while the measured lateral displacement Y_s gives the *feedback* correction to compute the curvature ρ^*.

Note that each transponder is unambiguously identified by a code, transmitted to the on board antenna, and that, by

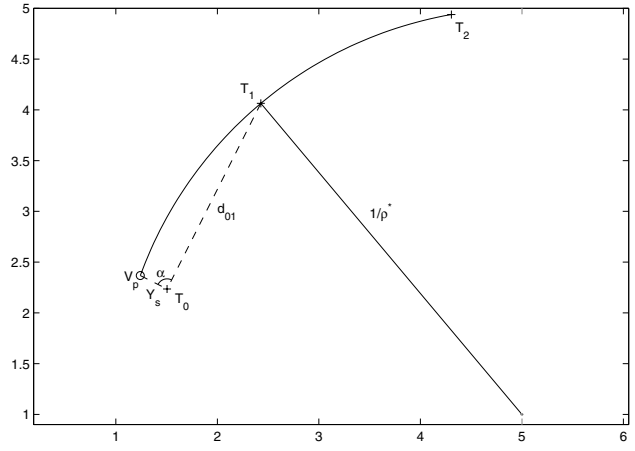

Fig. 5. Computation of corrected curvature ρ^*.

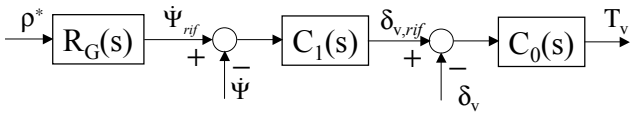

Fig. 6. Linear controller layout.

means of this code, many data associated to each transponder can be pre-computed and memorized in the vehicle ECU and used when needed. Among these data, absolute position coordinates $(X_t,\ Y_t)$ of the transponders, and distances between two consecutive transponders along the desired path, are used to compute the corrected curvature ρ^*, as described above.

Moreover, due to the particular plant configuration, that is to say, to the fact that the only information about the vehicle position is given by the interaction between a transponder and the on board antenna, the nonlinear controller can compute ρ^* only if at least one measure of Y_s has been obtained. Motivated by this consideration, at the start-up, we suppose that the vehicle begin to move along a straight section of the circuit, lined up and centered with the path to be followed so that the control algorithm set the steering wheel angle $\delta_v = 0$ until the first transponder is reached and a first value of Y_s is obtained. This is surely a limitation, but it is quite reasonable to suppose that, when a car stops in a parking area, the described situation will be the usual one.

The linear controller is depicted in Fig. 6. In this controller, a first inner loop is closed on the cascade compensator $C_0(s)$, using the measured steering wheel angle δ_v compared with a reference angle $\delta_{v,rif}$. This inner loop gives the command torque T_v. The filter $C_0(s)$ is a simple lead-lag, robustly designed to stabilize the loop, to minimize the steady state error and to satisfy the constraint given by the saturation limit on the command torque:

$$C_0(s) = 40\frac{(1+0.15s)\,(1+0.67s)}{(1+0.0167s)\,(1+10s)} \tag{7}$$

The reference angle $\delta_{v,rif}$ is the output of a second outer loop, closed on the cascade compensator $C_1(s)$, using the measured yaw rate $\dot{\Psi}$ compared with a reference yaw rate $\dot{\Psi}_{rif}$. The compensator $C_1(s)$ is a simple lag filter, designed to stabilize the loop and to minimize the steady state error:

$$C_1(s) = 150\frac{1+0.5s}{1+10s} \tag{8}$$

The reference yaw rate $\dot{\Psi}_{rif}$ is the output of the block $R_G(s)$, that is a low-pass filter with a static gain depending from the vehicle speed:

$$R_G(s) = \frac{1.2V_s}{1+0.25s} \tag{9}$$

The input of filter $R_G(s)$ is the corrected curvature ρ^*, computed by the nonlinear controller.

The nonlinear controller closes, through the measured signal Y_s, a third outer loop designed on the base of geometric considerations, as stated above. Of course the overall closed

loop stability has to be assured. In our case stability was checked at first by simulation, then by a direct test on the vehicle. Moreover, the analytical stability may be inferred from the following condition that holds for the system under consideration (the details are not reported for the sake of brevity).

Stability condition: the nonlinear closed loop system is asymptotically stable if and only if the non linearity $\rho^* = C_{nl}(Y_s)$ is sector bounded and it is differentiable at the system origin, that is to say for $Y_s = 0$.

IV. TEST CIRCUIT

The test circuit, used to check the designed compensator, actually represents a worst case of a urban context real situation. In fact, it is about 300 meters long and has markers (the transponders) placed at a distance of about 2 meters in straight sections and 1 meter in bend sections, as described in Fig. 7. Moreover, both left and right turns, which radius ranges between about 3 and 15 meters, can be found in the circuit connected by some straight sections, which maximum length is about 30 meters. Note that the circuit has a "common" section (X_t coordinate ranging about in the interval $0 \div 15$ m and Y_t coordinate about equal to 0 m) that is covered by the vehicle in both directions. The control algorithm is able to detect which is the followed direction by means of the pre-computed data associated to each transponder.

The presented control structure showed to be effective in simulation (here not presented) and when implemented on the vehicle ECU. In fact, the requested performance about the lateral displacement, that is to say, $|Y_s| \leq 0.25$ m to allow the transponders/antenna communication, was satisfied everywhere along the circuit. On the contrary, the robustness request, $|Y_s| \leq 0.10$ m, and the limit on the control effort, $|T_v| \leq 7$ Nm, that takes into account the actual saturation on the command torque, were not satisfied in many different part of the test circuit, [8].

It was clear, from an analysis of the acquired data, that one of the main problems in following the desired "ideal" path was the non perfect placement of the transponder along this path. This non perfect placement can be due to physical constraints, such as a minimum distance, between a transponder and a metallic mass or electric wires, needed to have no interferences in the transponders/antenna communication, or to scarce accuracy in making the hole in the asphalt to receive the transponder.

A solution was find in defining the "ideal" path as a series of sections, which length is maximized and which curvature is constant, and such to cover the whole test circuit. To define these sections, in correspondence to each actual transponder T, which position is given by the coordinates $(X_t,\ Y_t)$, a "virtual" transponder TV was defined by a pair of coordinates $(X_{tv},\ Y_{tv})$ belonging exactly to the ideal path and at a distance from the corresponding actual transponder less than a fixed value d_t.

More precisely, the "ideal" Test Circuit (TC) is defined as the union of different sections, such to cover the whole circuit, as follows:

$$TC \triangleq \bigcup_{i=1}^{M} \mathcal{S}_i \tag{10}$$

where $\mathcal{S}_i$ is the i-th section of the test circuit, defined as the set of the coordinates of the virtual transponders belonging to the section itself:

$$\mathcal{S}_i \triangleq \{(X_{tv,ij},\ Y_{tv,ij}),\ j = 1, \ldots, N_i\} \tag{11}$$

A generic section $\mathcal{S}_i$ is depicted in Fig. 8 and can be obtained by the following maximization problem:

$$\max N_i, \text{ subject to} \tag{12}$$

$$(X_{tv,ij} - X_{0,i})^2 + (Y_{tv,ij} - Y_{0,i})^2 = 1/\rho_i^2, \quad \forall j = 1, \ldots, N_i \tag{13}$$

$$d_{ttv,ij} < d_t, \quad \forall j = 1, \ldots, N_i \tag{14}$$

$$\text{with } d_{ttv,ij} = \sqrt{(X_{t,ij} - X_{tv,ij})^2 + (Y_{t,ij} - Y_{tv,ij})^2} \tag{15}$$

where (12) maximizes the number N_i of transponders belonging to the section $\mathcal{S}_i$ and therefore its length. Moreover,

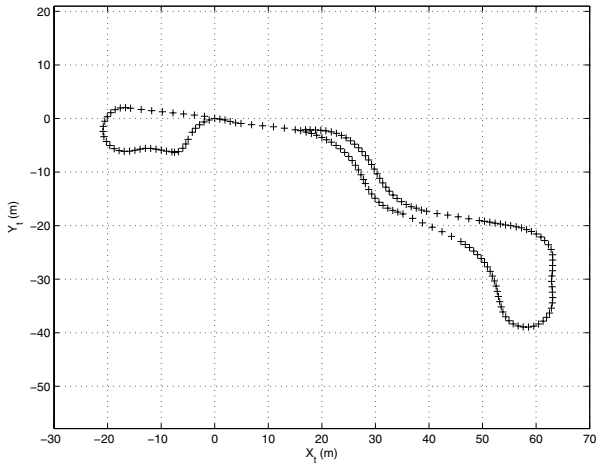

Fig. 7. Test circuit map with markers positions.

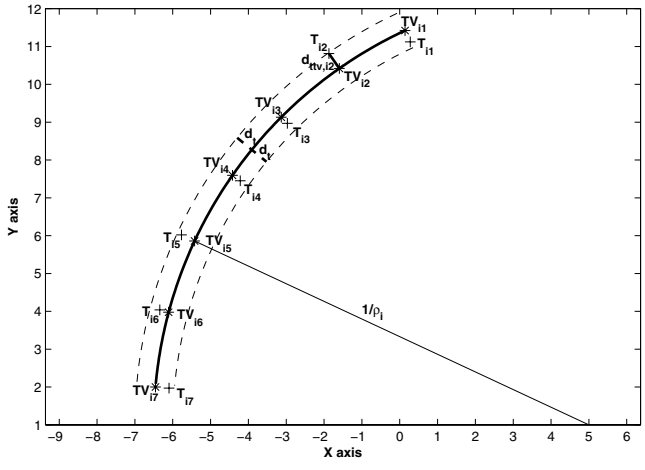

Fig. 8. Generic circuit section $\mathcal{S}_i$ with $N_i = 7$.

(13), (14) and (15) define the virtual transponder TV_{ij} positions, through their coordinates $(X_{tv,ij},\ Y_{tv,ij})$, belonging to a circle (13) centered in $(X_{0,i},\ Y_{0,i})$ with radius $1/\rho_i$, where ρ_i is the constant curvature of the circuit section, and at a distance (15) from the actual corresponding transponder less than d_t, (14). In other words, the whole circuit is approximated by a collection of circles that have distance from the actual transponders less than d_t.

In our case, the distance d_t can be conveniently chosen equal to 0.1 m, according to the antenna measure range.

V. TEST RESULTS

The presented control structure was modified to take into account the "ideal" path (10) simply by purging, in correspondence to each transponder, the measured lateral displacement Y_s from the pre-computed distance d_{ttv} (15) between the actual and the virtual transponders, and using this purged lateral displacement Y_s^* and the position of the virtual transponders in computing the corrected curvature ρ^*.

This way the control algorithm was more efficient. In order to show this effectiveness, some experimental results are reported. For the sake of clarity, these results are related only to a section of one lap of the test circuit, with vehicle moving, in counterclockwise direction, along the right part of the circuit, from the right end of the common section to the right most bends and back to the common section. Of course, similar results have been obtained either for the other part of the circuit, or repeating the lap, provided that, at start-up, the vehicle-path alignment conditions described in Section III are satisfied.

In Fig. 9 the bottom right bend of the circuit is shown: the "plus" signs correspond to the virtual transponder positions while the "circle" signs correspond to the vehicle positions. As it can be seen from this figure, the vehicle positions follow almost perfectly the "ideal" path markers.

In order to refer to the requested performances about the lateral displacement, that is to say, $|Y_s| \leq 0.25$ m to allow the transponders/antenna communication, in Fig. 10 the signal Y_s time behavior is plotted. It can be seen that this performance request is always satisfied, so that there are no missing transponders or, in other words, there is no gap in transponders/antenna communication. Note that in the showed time range the vehicle moved, as already said, along the right part of the circuit, while the part of the circuit shown in Fig. 9 refers only to the time interval $23 \div 31$ s, thus showing a subset of data of Fig. 10.

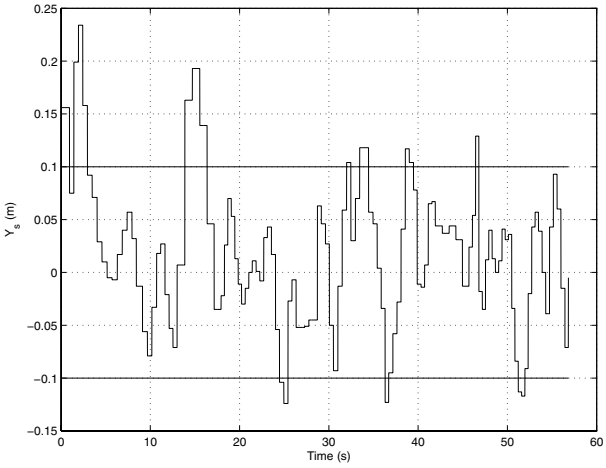

Fig. 10. Lateral displacement Y_s.

Moreover, the robustness request on the lateral displacement, that has now to be applied to the purged lateral displacement: $|Y_s^*| \leq 0.10$ m, is satisfied almost everywhere as showed in Fig. 11.

The other control performance requests to limit the control effort, taking into account the actual saturation on the command torque: $|T_v| \leq 7$ Nm. Fig. 12 shows the time behavior of the unsaturated signal T_v: it can be seen that, again, the performance is satisfied almost everywhere.

Fig. 10, 11 and 12 show that the control algorithm works in a effective way, even if it has to be slightly improved in order to satisfy the requested performances tightly. However, when command saturation at 7 Nm occurs, note that there

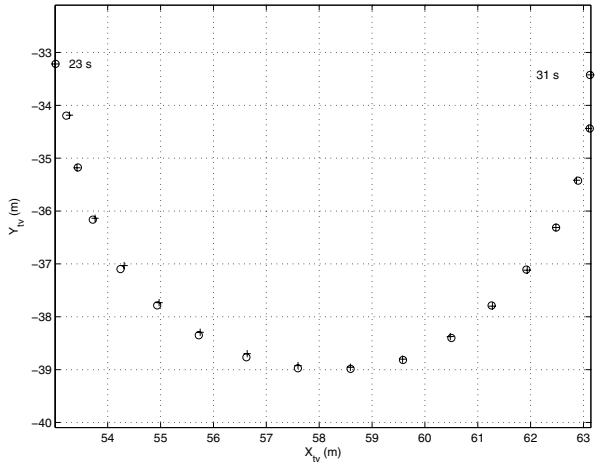

Fig. 9. Part of test circuit map with markers (+) and vehicle (o) positions.

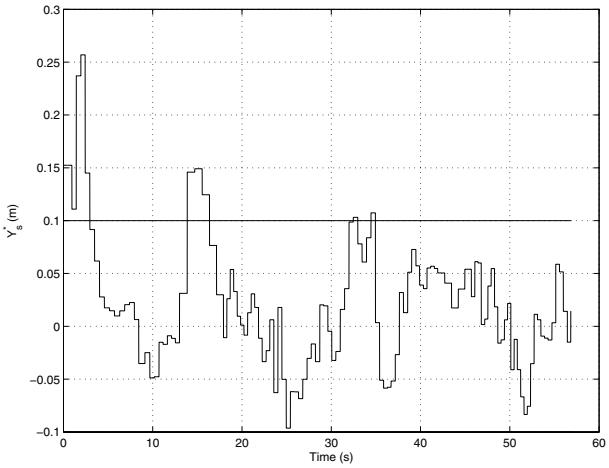

Fig. 11. Purged lateral displacement Y_s^*.

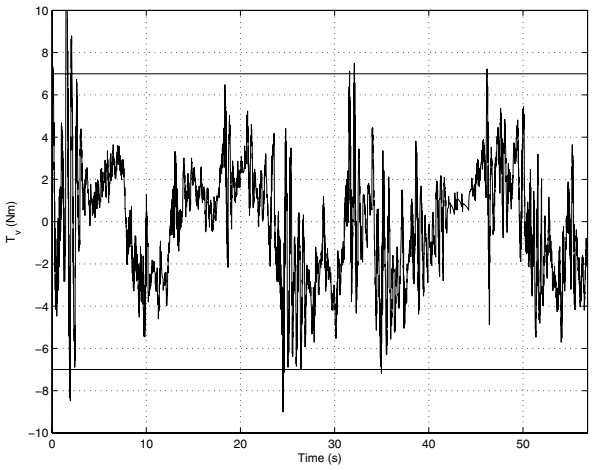

Fig. 12. Requested command torque T_v.

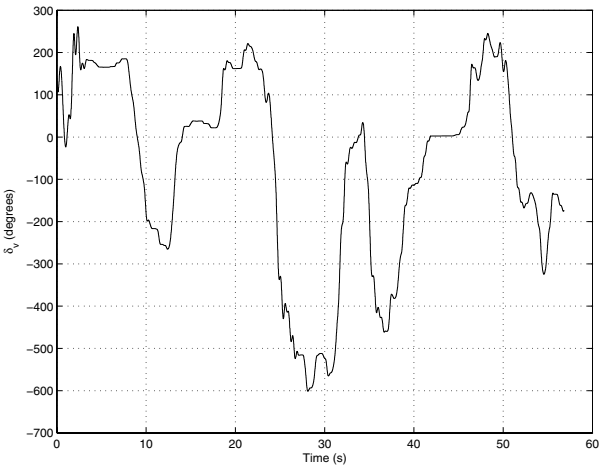

Fig. 13. Steering wheel angle δ_v.

are no problems in the controlled vehicle: no stability loose or excessive performance degradation. This way, there is no need of any particular control structure to avoid saturation, that is quite strictly linked to high values of lateral displacement. Higher values of command torque and/or wider saturation time intervals would imply antenna-transponder communication loose, that is to say the vehicle not following the desired path. This would mean a complete failure of the control algorithm and the need of its complete re-design.

Besides the control performance, also the steering wheel angle δ_v, plotted in Fig. 13, can be considered to evaluate the control algorithm. From this figure, it appears that the time behavior of this signal is quite smooth.

Eventually note that, during the presented test, the maximum vehicle speed was about 10 Km/h, thus reaching half of the allowed maximum speed of 20 Km/h. This is due to the continuous alternation of tight bends and very short straight sections of the test circuit. In future the controlled vehicle will be tested on a simpler circuit, in order to exploit the possibility to reach higher velocities.

A further problem, with economic and structural implications, that will be considered in future, is the possibility to use less transponders, that is to say, to install the transponders at a distance greater than 1 or 2 meters. This is not an easy problem due to the fact that the open loop plant (from the steering wheel torque T_v to the lateral displacement Y_s) is unstable and that the overall system, when there is no update in the lateral displacement measure, works with no feedback.

VI. CONCLUSIONS

In this paper we presented the lateral dynamic control of electric vehicles in a urban environment, motivated from individual public transportation issues, aimed to reduce metropolitan areas pollution.

The presented framework consider a "Look-Down" reference, because the lateral displacement is obtained from a on board antenna interacting with transponders, used as road markers.

Results from experimental tests, of the designed control strategy, performed on an actual circuit showed the effectiveness of the considered control strategy.

Some improvements of the control algorithm are still needed, in order to satisfy the requested performances tightly.

REFERENCES

[1] S. A. Nobe and F. Y. Wang, "An overview of recent developments in automated lateral and longitudinal vehicle controls," in *Proceedings of the IEEE International Conference on Systems, Man and Cybernetics*, 2001, pp. 3447–3452.

[2] S. E. Shladover, C. A. Desoer, J. K. Hedrick, M. Tomizuka, J. Walrand, W. Zhang, D. H. McMahon, H. Peng, S. Sheikholeslam, and N. McKeown, "Automatic vehicle control developments in the PATH program," *IEEE Transactions on vehicular technology*, vol. 40, no. 1, pp. 114–130, February 1991.

[3] R. Garcia, T. de Pedro, J. Naranjo, J. Reviejo, and C. Gonzalez, "Frontal and lateral control for unmanned vehicles in urban tracks," in *Proceedings of IEEE Intelligent Vehicle Symposium*. Versailles, France: IEEE, June 2002, pp. 583–588.

[4] S. I. Eom, E. J. Kim, T. Y. Shin, M. H. Lee, and F. Harashima, "The robust controller design for lateral control of vehicles," in *Proceedings 2003 IEEE/ASME International Conference on Advanced Intelligent Mechatronics*. Kobe, Japan: IEEE, July 2003, pp. 570–573.

[5] T. H. Chang, "Field performance assessment of the ADVANCE-F automatic steering control vehicle," *Control engineering practice*, no. 12, pp. 569–576, 2004.

[6] J. Hernandez and C. Kuo, "Lateral control of higher order nonlinear vehicle model in emergency maneuvers using absolute positioning GPS and magnetic markers," *IEEE Transactions on Vehicular Technology*, vol. 53, no. 2, pp. 372–384, March 2004.

[7] S. Chaib, M. Netto, and S. Mammar, "$H_{\inf}$, adaptive, PID and fuzzy control: A comparison of controllers for vehicle lane keeping," in *Proceedings of IEEE Intelligent Vehicles Symposium*. Parma, Italy: IEEE, June 2004, pp. 139–144.

[8] S. Malan, M. Milanese, P. Borodani, and A. Gallione, "Lateral control of autonomous vehicle for public urban mobility systems," in *Proceedings of the 8th International IEEE Conference on Intelligent Transportation Systems*, Wien, Austria, September 2005.

[9] S. Shladover, D. Wormley, H. Richardson, and R. Fish, "Steering controler design for automated guideway transit vehicles," *ASME journal of dynamic systems, measurement and control*, vol. 100, pp. 1–8, March 1978.

[10] M. Tomizuka, "Computer control of vehicles: Overcoming limitations of human drivers," in *Control and Modeling of Complex Systems*, ser. Trends in Mathematics, Hashimoto, Oishi, and Yamamoto, Eds. Birkhäuser, 2003, pp. 283–301.